

^{13}C and ^{15}N NMR Mechanistic Study of Cyanide Exchange on Oxotetracyanometalate Complexes of Re(V), Tc(V), W(IV), Mo(IV), and Os(VI)

Amira Abou-Hamdan,¹ Andreas Roodt,^{*,2} and André E. Merbach^{*,1}

Institut de Chimie Minérale et Analytique, Université de Lausanne, Bâtiment de Chimie (BCH), Lausanne CH-1015, Switzerland, and Department of Chemistry, University of the Orange Free State, Bloemfontein 9300, South Africa

Received September 30, 1997

A range of complexes with general formula $[\text{MO}(\text{X})(\text{CN})_4]^{n-}$ of W(IV), Mo(IV), Re(V), Tc(V), and Os(VI) were prepared and characterized by ^{13}C , ^{15}N , ^{17}O , and ^{99}Tc NMR, utilizing ^{13}C - and ^{15}N -enriched cyano complexes. A correlation between M–O and M–CN bond strength from X-ray crystallographic data and $|^1J(^{183}\text{W}-^{13}\text{C})|$ coupling is reported. The cyanide (HCN/CN⁻) exchange kinetics on the *trans*-dioxotetracyanometalate complexes and protonated/substituted ($[\text{MO}(\text{X})(\text{CN})_4]^{n-}$) forms thereof were studied in aqueous medium. The dioxotetracyano complexes show a trend of reactivity $\text{M(IV)} > \text{M(V)} > \text{M(VI)}$, which is in agreement with the increase in M–L bond strength (L = O²⁻ or CN⁻) and a dissociative activation for the cyanide and the oxygen exchange in these complexes. Rate constants (X, k_{Xc}) in s⁻¹ at 298 K for the $[\text{MO}(\text{X})(\text{CN})_4]^{n-}$ complexes are as follows for Mo(IV): O²⁻, >0.4; OH⁻, $(1.7 \pm 0.1) \times 10^{-2}$; H₂O, $(1.5 \pm 0.1) \times 10^{-2}$; CN⁻, $(9.6 \pm 0.8) \times 10^{-3}$. For W(IV): O²⁻, $(4.4 \pm 0.4) \times 10^{-3}$; OH⁻, $(9.6 \pm 0.9) \times 10^{-5}$; H₂O, $(1.1 \pm 0.1) \times 10^{-4}$; CN⁻, $(1.1 \pm 0.1) \times 10^{-2}$; N₃⁻, $(3.1 \pm 0.2) \times 10^{-4}$; F⁻, $(4.8 \pm 0.1) \times 10^{-5}$. For Tc(V): O²⁻, $(4.8 \pm 0.4) \times 10^{-3}$; H₂O, $<4 \times 10^{-5}$; NCS⁻, $<4 \times 10^{-5}$. For Re(V): O²⁻, $(3.6 \pm 0.3) \times 10^{-6}$ and $(1.2 \pm 0.1) \times 10^{-4}$ for CN⁻ and HCN, respectively; OH₂, $<4 \times 10^{-8}$. For Os(VI): O²⁻, $<4 \times 10^{-9}$ and $(1.2 \pm 0.1) \times 10^{-4}$ for CN⁻ and HCN, respectively. The cyanide exchange kinetics were correlated with previously determined proton and oxygen exchange, spanning a kinetic domain of more than 12 orders of magnitude for the five metal centers studied.

Introduction

The substitution and protonation behavior of the dioxotetracyanometalate complexes of Re(V), Tc(V), W(IV), and Mo(IV) have been extensively investigated in the past decade³ and have recently been reviewed.⁴ We have in the course of these investigations selected these oxygen/cyano-containing complexes for a systematic study with regard to ligand, water, and proton kinetic exchange studies, utilizing ^{17}O and ^{13}C NMR for this purpose.^{5–7} We have furthermore reported the characterization of these oxo complexes with NMR and were able

to correlate chemical shifts and acid/base behavior with structural and infrared data.

The equilibria governing the complex formation and oxygen and proton exchange in these systems are given by Scheme 1, where CN denotes the total free cyanide, i.e., HCN/CN⁻, and will be used as such throughout this work. In the complex formation (eq 2) X represents different entering nucleophiles such as NCS⁻, F⁻, and CN⁻.

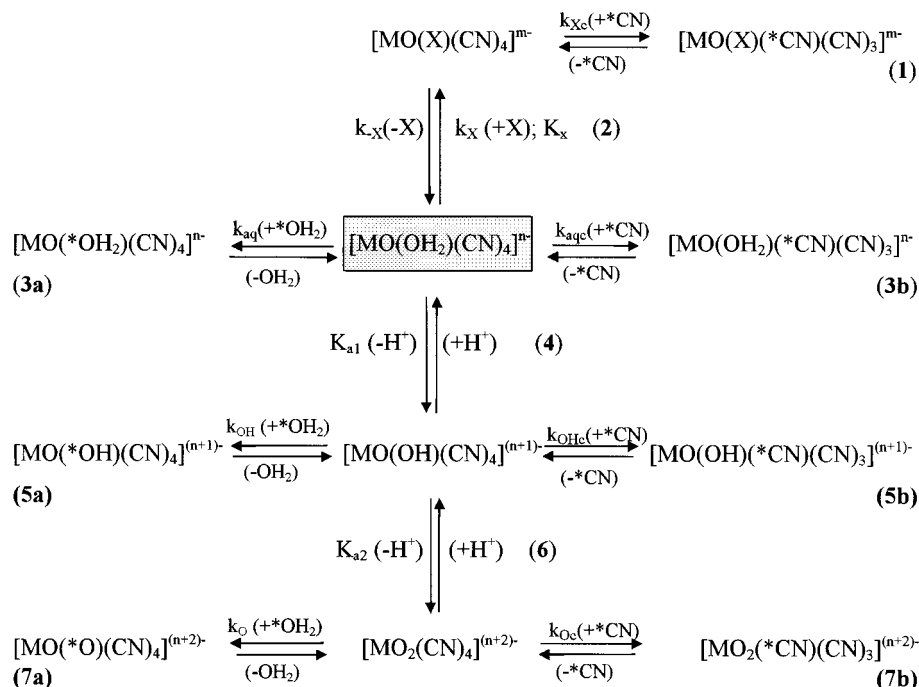
We have determined the proton exchange rate constants⁶ in the above scheme, and therefore elucidated the mechanisms of the kinetics for the reactions given in eqs 4 and 6, and we have shown that the proton exchange in these complexes can proceed via protolysis, hydrolysis, and direct proton exchange. Furthermore, we have established that the enrichment of the oxo oxygen in both $[\text{MO}(\text{OH})(\text{CN})_4]^{(n+1)-}$ and $[\text{MO}(\text{OH})_2(\text{CN})_4]^{n-}$ proceeds *via* the dioxo species in Scheme 1 after rapid exchange between the bulk H₂*O and the coordinated aqua ligand, reaction 3a acting as a “bottleneck” in this process.

We have also recently reported the oxygen exchange kinetics⁷ of the complexes shown in Scheme 1 in reactions 3a, 5a, and 7a, utilizing ^{17}O NMR and correlating the results obtained with those of previous proton exchange studies to describe the

- (1) Université de Lausanne.
 (2) University of the Orange Free State.
 (3) (a) Roodt, A.; Leipoldt, J. G.; Deutsch, E. A.; Sullivan, J. C. *Inorg. Chem.* **1992**, *31*, 1080. (b) Roodt, A.; Leipoldt, J. G.; Basson, S. S.; Potgieter, I. M. *Transition Met. Chem.* **1988**, *13*, 336. (c) Roodt, A.; Leipoldt, J. G.; Basson, S. S.; Potgieter, I. M. *Transition Met. Chem.* **1990**, *15*, 439. (d) Potgieter, I. M.; Basson, S. S.; Roodt, A.; Leipoldt, J. G. *Transition Met. Chem.* **1988**, *13*, 209. (e) Purcell, W.; Roodt, A.; Basson, S. S.; Leipoldt, J. G. *Transition Met. Chem.* **1989**, *14*, 224. (f) Purcell, W.; Roodt, A.; Leipoldt, J. G. *Transition Met. Chem.* **1991**, *17*, 339. (g) Purcell, W.; Roodt, A.; Basson, S. S.; Leipoldt, J. G. *Transition Met. Chem.* **1989**, *14*, 369. (h) Roodt, A.; Basson, S. S.; Leipoldt, J. G. *Polyhedron* **1994**, *13*, 599. (i) Smit, J. P.; Purcell, W.; Roodt, A.; Leipoldt, J. G. *Polyhedron* **1993**, *12*, 2271. (j) Smit, J. P.; Purcell, W.; Roodt, A.; Leipoldt, J. G. *J. Chem. Soc., Chem. Commun.* **1993**, *18*, 1388. (k) Purcell, W.; Roodt, A.; Leipoldt, J. G. *Transition Met. Chem.* **1993**, *18*, 1388. (l) Leipoldt, J. G.; van Eldik, R.; Basson, S. S.; Roodt, A. *Inorg. Chem.* **1986**, *25*, 4639. (m) Damoense, L. J.; Purcell, W.; Leipoldt, J. G. *Transition Met. Chem.* **1994**, *19*, 619.
 (4) Leipoldt, J. G.; Basson, S. S.; Roodt, A. *Advances in Inorganic Chemistry*; Sykes, A. G., Ed.; Academic Press: Orlando, FL, 1993; Vol. 40, p 242. (b) Leipoldt, J. G.; Basson, S. S.; Roodt, A.; Purcell, W. *Polyhedron* **1992**, *11*, 2277.

- (5) Roodt, A.; Leipoldt, J. G.; Helm, L.; Merbach, A. E. *Inorg. Chem.* **1992**, *31*, 2864.
 (6) Roodt, A.; Leipoldt, J. G.; Helm, L.; Merbach, A. E. *Inorg. Chem.* **1994**, *33*, 140.
 (7) Roodt, A.; Leipoldt, J. G.; Helm, L.; Abou-Hamdan, A.; Merbach, A. E. *Inorg. Chem.* **1995**, *34*, 350.

Scheme 1



dynamic behavior of the coordination polyhedron upon oxo protonation as a function of pH, over a range of ten orders of magnitude.

In this paper we report the cyanide exchange on the complexes as described by reactions 1, 3b, 5b, and 7b in Scheme 1 and correlate them with the above-mentioned proton and oxygen exchange dynamics of these cyano complexes.

Experimental Section

General Considerations. *Caution:* Technetium-99 emits a low-energy (0.292 MeV) β -particle with a half-life of 2.12×10^5 years. However, when this material is handled in milligram amounts it does not present any serious health hazard since ordinary laboratory glassware and other materials provide adequate shielding. Bremsstrahlung is not a significant problem due to the low energy of the β -particle emission, but normal radiation safety procedures must be used at all times, especially when handling solid samples, to prevent contamination and possible inhalation. Also beware of hydrogen cyanide gas in all of the following syntheses and manipulations.

Unless otherwise noted, all chemicals were of reagent grade and all experiments were performed aerobically. 10% ^{17}O -enriched water was purchased from Enrichment Ltd, catalog no. NW-17-10; NaC^{15}NS (99%) was from Dr Glaser AG Basel; and K^{13}CN (99%) and NaC^{15}N (98%) were from Cambridge Isotope Laboratories.

Preparation of Complexes. $\text{K}_3\text{Na}[\text{MoO}_2(\text{CN})_4] \cdot 6\text{H}_2\text{O}$, $\text{K}_3\text{Na}[\text{WO}_2(\text{CN})_4] \cdot 6\text{H}_2\text{O}$, $\text{K}_3[\text{ReO}_2(\text{CN})_4]$, and $\text{K}_2[\text{OsO}_2(\text{CN})_4]$ were prepared as described previously.³

^{13}C - or ^{15}N -Enriched Complexes of $\text{K}_3\text{Na}[\text{MO}_2(\text{CN})_4] \cdot 6\text{H}_2\text{O}$ [$\text{M} = \text{Mo}(\text{IV})$, $\text{W}(\text{IV})$]. Approximately 100 mg of complex was dissolved in water followed by the addition of ca. 40 mg of the enriched cyanide salt. After about 1 h, the complex was precipitated by the slow addition of KOH (0.5 g), NaOH (0.2 g), and ethanol. The solid was decanted, washed three times with ethanol solutions saturated with KOH , and dried in a fume hood. The products were characterized as described before.³

^{13}C - or ^{15}N -Enriched Complexes of $\text{K}_3[\text{MO}_2(\text{CN})_4]$ [$\text{M} = \text{Tc}(\text{V})$ or $\text{Re}(\text{V})$]. Approximately 100 mg of complex was dissolved in water followed by the addition of ca. 40 mg of the enriched cyanide salt. The exchange in the $\text{Tc}(\text{V})$ complex was completed in less than 10 min at room temperature, whereas the $\text{Re}(\text{V})$ complex had to be heated

at ca. 50 °C for ca. 2 h to ensure exchange equilibrium. The enriched complexes were precipitated by addition of methanol, washed, and dried in air. The products were characterized as described before.³

Preparation of $[\text{MO}(\text{CN})_5]^{n-}$ and $[\text{MO}(\text{X})(\text{CN})_4]^{n-}$ Solutions. (a) For preparation of the $[\text{MO}(\text{CN})_5]^{n-}$ solutions, a solution of 0.2 m (throughout the text m represents molal = moles per kg) of the corresponding dioxotetracyanometalate complex and 0.3 m of K^{13}CN adjusted to pH ca. 9 was used. (b) For preparation of the $[\text{MO}(\text{X})(\text{CN})_4]^{n-}$ solutions, a solution mixture of 0.2–2 m of X (X = KF , NaN_3 , KNCS , py) and 0.2 m of the dioxotetracyanometalate complex acidified to pH ca. 6 was used. (c) For preparation of the $[\text{MO}(\text{OH}_2)(\text{CN})_4]^{2-}$ ($\text{M} = \text{W}$, Mo) solutions,^{3,1j} a $[\text{MO}_2(\text{CN})_4]^{4-}$ solution acidified to pH ca. 6.5 was used.

pH Measurements. A combined Calomel electrode from Radiometer (GK2322C) and Metrohm Herisau E603 and 692 pH meters were calibrated with standard HNO_3 and decarbonated NaOH solutions in the usual way, incorporating the variation in the ion product of water as a function of both ionic strength and temperature.⁸ Secondary buffers were also used for standardization at intermediate pH values [potassium hydrogen phthalate (4.00), potassium dihydrogen phosphate and disodium hydrogen phosphate (6.85–6.88), and sodium tetraborate (9.10–9.20)], with the pH defined as $-\log[\text{H}^+]$.

NMR Measurements. The NMR experiments were done on Bruker AC-200 (cryomagnet 4.7 T), at 50.3 MHz (^{13}C), and 45.10 MHz (^{99}Tc), Bruker AM-400 and ARX-400 (cryomagnet 9.4 T), at 100.6 MHz (^{13}C), 40.6 MHz (^{15}N), and 54.25 MHz (^{17}O), and Bruker AMX-2 600 (cryomagnet 14.1 T) spectrometers at 150.90 MHz (^{13}C) and 60.81 MHz (^{15}N). The ^{17}O shifts were referenced to the water peak and measured with respect to the nitrate ion, $\delta(\text{NO}_3^-) = 413$ ppm, as internal reference.⁶ All aqueous solutions used for ^{17}O measurements contained 5% ^{17}O -enriched water. The ^{13}C shifts were measured with respect to external $[\text{Re}_2\text{O}_3(^{13}\text{C})_8]^{4-}$ ($\delta = 134$ ppm) as described previously,⁵ while the ^{15}N shifts were referenced relative to nitromethane⁹ ($\delta = 0$ ppm) and measured using external 5 M NaC^{15}N ($\delta = -106.3$ ppm). All aqueous solutions used for ^{13}C and ^{15}N measurements contained 2% D_2O as internal lock substance. The ^{99}Tc shifts were measured

(8) Smith, R. M.; Martell, A. E. *Critical Stability Constants*; Plenum Press: New York, 1974; Vol. 4, p 1.

(9) Levy, G. C.; Lichter, R. L. *Nitrogen-15 Nuclear Magnetic Resonance Spectroscopy*; John Wiley & Sons, Inc.: New York, 1979; p 30.

relative to $\text{NH}_4^{99}\text{TcO}_4$ as external standard ($\delta = 0$ ppm).¹⁰ The temperature was controlled by a Bruker B-VT 1000 unit and was measured by substituting the sample tube for one containing a Pt-100 resistor.¹¹ Unless otherwise stated in the figure headings, the parameters for the collection of ^{17}O NMR spectra were the following: a frequency range of 50 kHz was used to collect 2K data points with a pulse length of 14 μs and an exponential line broadening of 80 Hz. The time between transients, of which 10 000 were added prior to Fourier transformation, was 0.1 s. The parameters for the collection of ^{13}C NMR spectra for the kinetic isotopic exchange studies were the following: frequency range, 29.4 kHz; 8K data points collected; pulse length, 20 μs ; exponential line broadening, 8 Hz. The time between transients, of which between 4 and 36 were added prior to Fourier transformation, was 60 s. The longitudinal relaxation time values T_1 , in s, were determined for the $[\text{ReO}_2(\text{CN})_4]^{3-}$ complex, using the inversion recovery pulse sequence, for the bound and free cyanide at 297.9, 307.2, and 333.8 K are 1.02, 11.48; 1.19, 10.98; and 1.83, 8.59, respectively; thus, RD was fixed as 60 s (ca. $5T_1$) for the ^{13}C kinetic runs. The data collection parameters in the ^{15}N kinetic isotopic exchange studies were the following: frequency range, 4.2 kHz; 16K data points collected; pulse length, 20 μs ; exponential line broadening, 0.2 Hz. Again, the time between transients, of which between 4 and 36 were added prior to Fourier transformation, was 6–60 s.^{12a} The parameters for the data collection of ^{99}Tc NMR spectra were the following: frequency range, 100 kHz; collect 8K data points collected; pulse length, 20 μs ; exponential line broadening, 8 Hz. The time between transients, of which 100 were added prior to Fourier transformation, was 1 s.

Kinetics and Data Treatment. The slow isotopic exchange in a chemical system, as, for example, the reaction of a metal complex containing exchangeable cyano ligands, can be followed by monitoring the bound ^{13}C or ^{15}N NMR signal growth as a function of time. For the kinetic runs a preweighed sample of the relevant metal complex was dissolved in thermostated water at the required pH (in the cases of $[\text{MO}(\text{CN})_5]^{m-}$ and $[\text{MO}(\text{X})(\text{CN})_4]^{m-}$, see solution preparations above), followed by the addition of $^{13}\text{C}/^{15}\text{N}$ potassium/sodium cyanide, also at the required pH, to the mixture, introduction of the sample in a 10 mm NMR tube, and immediate commencement of the data collection. All measurements were performed on solutions with total metal complex concentration of 0.1–0.2 m at ionic strength of 1.2 m (KCl/KNO_3 as supporting electrolyte) unless otherwise stated. A selective variation of the metal complex concentration by a factor of up to 2 showed no influence on the NMR-observed exchange rate constants in these systems.

Variable cyanide concentration NMR measurements for the $\text{K}_3\text{ReO}_2(\text{CN})_4$ complex were done at pH = 11 in the temperature range 307–332 K with total metal concentration of 0.2 m and KCN concentration ranging from 0.3 to 1.6 m (corresponding ionic strength of 1.5–2.8 m). Another variable concentration cyanide exchange study, also ranging from 0.3 to 1.6 m, was carried out at pH = 5.7. The variable pH study was done at 298 K with total metal concentration of 0.2 m and KCN concentration of 0.3 m in the pH range of 1.0–11.3 for the $\text{Re}(\text{V})$ complex (corresponding ionic strength of ca. 1.5 m).

(10) (a) Franklin, K. J.; Lock, C. J.; Sayer, B. G.; Schröbilgen, G. J. *J. Am. Chem. Soc.* **1982**, *104*, 5303. (b) O'Connell, L. A.; Pearlstein, R. M.; Davison, A.; Thornback, J. R.; Kronauge, J. F.; Jones, A. *Inorg. Chim. Acta* **1989**, *161*, 39. (c) Nicholson, T.; Mahmood, A.; Jones, A.; Davison, A. *Inorg. Chim. Acta* **1991**, *179*, 53.

(11) Ammann, C.; Meier, P.; Merbach, A. E. *J. Magn. Reson.* **1982**, *46*, 319.

(12) (a) Due to the cyanide exchange rate, the time between transients (RD) could not be taken as $5T_1 = 70$ s and a smaller relaxation delay was chosen (6s). In this case, the optimized pulse width corresponded to an Ernst angle of 60° (ref: Martin, M. L.; Delpuech, J.-J.; Martin, G. J. *Practical NMR Spectroscopy*; Heyden & Son Ltd: London, 1980; p 106). At the end of the kinetic runs, a spectrum was taken with RD = 70 s, a correction factor was thus calculated and applied to the integrated mole fractions. This allowed us to verify that x_∞ corresponds to the value expected from the solution preparation. (b) Helm, L.; Elding, L. I.; Merbach, A. E. *Inorg. Chem.* **1985**, *24*, 1719. (c) Helm, L.; Deutsch, K.; Deutsch, E.; Merbach, A. E. *Helv. Chim. Acta* **1992**, *75*, 210.

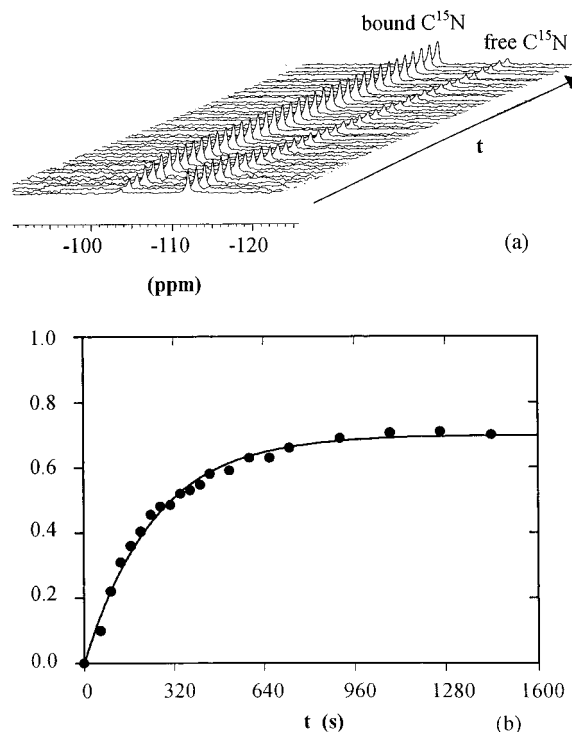


Figure 1. Slow $^{15}\text{N}^-$ isotopic exchange on $[\text{TcO}_2(\text{CN})_4]^{3-}$. (a) ^{15}N NMR spectra illustrating the signal growth of the $[\text{TcO}_2(^{15}\text{N})_4]^{3-}$ complex as a function of time and the corresponding decrease in the free $^{15}\text{N}^-$. (b) Least-squares fit of the data to eq 9. $[\text{Tc}(\text{V})]_{\text{tot}} = 0.17$ m; $[\text{C}^{15}\text{N}]_{\text{tot}} = 0.3$ m; pH = 10.6; $T = 279.2$ K.

The kinetics for the ^{15}N and ^{13}C isotopic exchange reactions (Scheme 1) can be expressed by the McKay equation^{12b,c,13} as given in eq 8 (the kinetic isotopic effects, probably never larger than 2%, have been neglected). In eq 8, k_{obs} represents the rate constant for the exchange

$$-dx/dt = k_{\text{obs}}(x - x_\infty)/(1 - x_\infty) \quad (8)$$

of a particular CN^- molecule and x and x_∞ are the mole fractions of bound molecule at the time of sampling and at exchange equilibrium, respectively. The time dependence of x , obtained from the integration of the bound and free signals, $x = I_{\text{bound}}/(I_{\text{bound}} + I_{\text{free}})$, where I represents the integral of the appropriate peak, was fitted to eq 9, resulting from the integration of eq 8 with $x = x_0$ at $t = 0$ and $x = x_\infty$ at $t = \infty$. The

$$x = x_\infty + (x_0 - x_\infty)\exp[-k_{\text{obs}}t/(1 - x_\infty)] \quad (9)$$

adjustable parameters were k_{obs} , x_0 , and x_∞ . A typical example of the ^{15}N -bound cyanide signal increase observed with time for the $\text{Tc}(\text{V})$ complex is shown in Figure 1, where the line represents the least-squares fit of the data to eq 9.

Results

NMR Characterization of Complexes. General Considerations. ^{13}C NMR was utilized to study different aspects of the reactivity of the systems as a function of certain structural aspects in the selected oxocyno complexes of $\text{Mo}(\text{IV})$, $\text{W}(\text{IV})$, $\text{Tc}(\text{V})$, $\text{Re}(\text{V})$, and $\text{Os}(\text{VI})$. The NMR spectral properties were typical as obtained from ^{13}C NMR in general, i.e., very sharp lines indicative of fairly long relaxation times on the order of a few seconds. Whereas in the case of $\text{Tc}(\text{V})$ the significant quadrupolar moment of the $\text{Tc}-99$ nucleus ($I = 9/2$, 100%

(13) Lincoln, S. F.; Merbach, A. E. *Advances in Inorganic Chemistry*; Sykes, A. G., Ed.; Academic Press: San Diego, CA, 1995; p 15.

(14) Day, V. W.; Hoard, J. *Am. Chem. Soc.* **1968**, *90*, 3374.

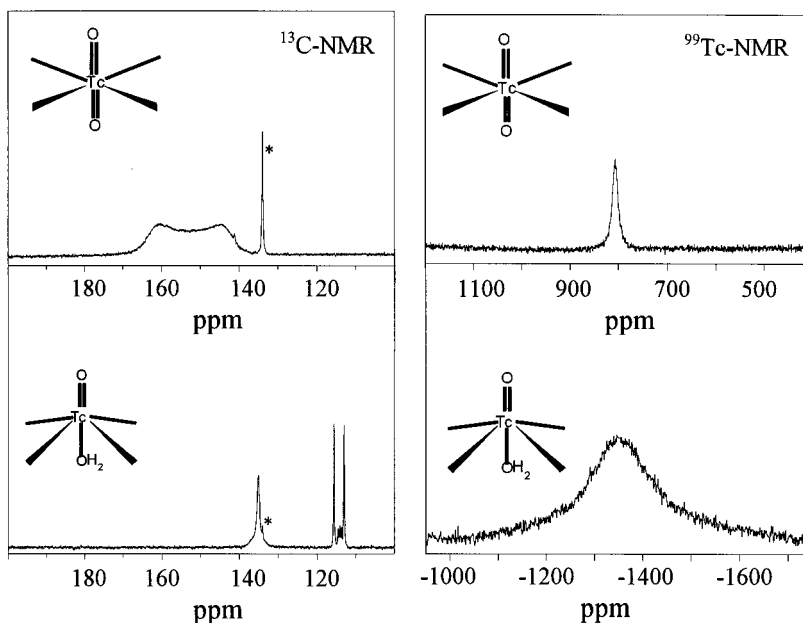


Figure 2. ^{13}C and ^{99}Tc NMR spectra at $T = 25\text{ }^\circ\text{C}$ of $[\text{TcO}_2(^{13}\text{CN})_4]^{3-}$ ($[\text{Tc(V)}]_{\text{tot}} = 0.12\text{ m}$; $\text{pH} = 8.0$) and $[\text{TcO}(\text{H}_2\text{O})(\text{CN})_4]^-$ ($[\text{Tc(V)}]_{\text{tot}} = 0.12\text{ m}$; $[\text{CN}]_{\text{tot}} = 0.83\text{ m}$; $\text{pH} = 1.0$); note the signal structure of the free HCN due to proton-carbon and deuterium-carbon couplings, illustrating the quadrupolar effect introduced by ^{99}Tc ($I = 1/2$, 100%) and the effect of reduced symmetry upon protonation, i.e., formation of the oxo aqua complex. The asterisked signal is the $[\text{Re}_2\text{O}_3(\text{CN})_8]^{4-}$ reference.

abundance)¹⁰ led to a very broad bound ^{13}C signal (partially quadrupole-collapsed decet having a line width of 2.5 kHz, estimated $1/T_{2Q}$ ca. 1500 s^{-1} , and $|^1J(^{99}\text{Tc}-^{13}\text{C})|$ ca. 200 Hz) at 153 ppm overlapping that of the free ^{13}C cyanide signal excluding the study of the cyanide exchange by ^{13}C NMR (see Figure 2 and discussion below). The exchange was then conveniently studied by ^{15}N ($I = 1/2$) NMR using ^{15}N -enriched cyanide, since the indirect scalar coupling constant $|^2J(^{15}\text{N}-^{99}\text{Tc})|$ is smaller than $|^1J(^{13}\text{C}-^{99}\text{Tc})|$.

Tungsten(IV) and Molybdenum(IV). The first-order couplings between the ^{13}C and the ^{183}W ($I = 1/2$; 14.4% natural abundance)¹³ nuclei for a range of different ligands X in the $[\text{WO}(\text{X})(\text{CN})_4]^{n-}$ complexes were studied and are illustrated in Figure 3 for the $[\text{WO}(\text{CN})_5]^{3-}$, $[\text{WO}(\text{H}_2\text{O})(\text{CN})_4]^{2-}$, and $[\text{WO}(\text{F})(\text{CN})_4]^{3-}$. The data for a range of $[\text{WO}(\text{X})(\text{CN})_4]^{n-}$ complexes are reported in Table 1. These couplings are correlated with the observed bond distances in selected complexes of this type and also with stability constants as obtained from complex formation studies. The Mo(IV) complexes studied were limited, but the details of those investigated are reported in Table 1.

Rhenium(V) and Technetium(V). The ^{13}C spectrum characteristics of the dioxo, hydroxo oxo, and aqua oxo tetracyano complexes of Re(V) as well as the dinuclear species, $[\text{Re}_2\text{O}_3(\text{CN})_8]^{4-}$, have been reported previously (also in Table 2). The ^{15}N chemical shift data obtained in this study for some of the Re(V) and Tc(V) complexes are reported in Table 3.

The ^{13}C NMR spectrum of ^{13}C -enriched dioxotetracyano-technetate(V) is shown in Figure 2, illustrating the substantial coupling with the ^{99}Tc ($I = 1/2$) nucleus. However, it is relaxed significantly upon protonation, forming the $[\text{TcO}(\text{H}_2\text{O})(\text{CN})_4]^-$ complex (see Figure 2). Furthermore, the ^{99}Tc spectra of the $[\text{TcO}_2(\text{CN})_4]^{3-}$ and $[\text{TcO}(\text{H}_2\text{O})(\text{CN})_4]^-$ complexes are given in Figure 2; the substantial broadening introduced by the double protonation of one oxo ligand (reactions 4 and 6, Scheme 1), as well as the significant shielding of the nucleus, is worth noting.

Table 1. Correlation between Equatorial Cyanide ^{13}C NMR and X-ray Data for $\text{trans-}[\text{WO}(\text{X})(\text{CN})_4]^{m-}$ Complexes

ligand X	$\delta^{13}\text{C}$ (ppm)	$^1J(^{183}\text{W}-^{13}\text{C})$ (Hz)	K_x^a	$\text{p}K_x$	bond distance (\AA)	
					W-CN ^b	Mo-CN ^b
O^{2-}	166	128	—	—	2.177(7) ^f	2.20(1) ^e
CN^{-c}	145	22	—	—	2.362(5) ^e	2.373(6) ^f
	(154) ^d					
OH^-	162	132	—	—	—	2.11(1) ^j
CN^-	151.9	133	1000	3.0	2.154(6) ^f	2.18(1) ^j
	(160) ^d		(100) ^d	(2.0) ^d		
F^-	160.5	134	150	2.2	2.14(2) ^g	—
N_3^-	157	135	48	1.7	—	2.17(2) ^k
NCS^-	158.7	135	2.0	0.30	2.14(3) ^h	—
py	159	136	0.27	-0.57	—	2.164(6) ^l
OH_2	159	136	—	—	—	2.16(1) ^j

^a Stability constant for $\text{trans-}[\text{WO}(\text{X})(\text{CN})_4]^{m-}$ complexes,¹⁵ as defined in Scheme 1. ^b Average equatorial W-CN distances from crystal structures. ^c Trans to oxo. ^d Data for the $[\text{MoO}(\text{CN})_5]^{3-}$ complex. ^e Reference 14. ^f Reference 15. ^g Reference 18. ^h Reference 3c. ⁱ Reference 16. ^j Reference 17. ^k Reference 19. ^l Reference 20.

Osmium(VI). The investigation of the chemical shifts for the Os(VI) was limited to the dioxotetracyano complex and is reported in Table 2. A first-order coupling between the ^{192}Os ($I = 1/2$, natural abundance = 1.64%) and ^{13}C was observed and is also reported in Table 2.

Exchange Kinetics. Rate Law for Cyanide Exchange. The cyanide exchange reactions on the metal centers in this study are presented in eqs 1, 3b, 5b, and 7b. Thus, the general rate law given in eq 10 describes cyanide exchange of the complete scheme. In eq 10, $[\text{MX}]$, $[\text{MOH}_2]$, $[\text{MOH}]$, and $[\text{MO}_2]$ represent

$$d[\text{M}^*\text{CN}]/dt = (k_{x\text{c}}[\text{MX}] + k_{\text{aqc}}[\text{MOH}_2] + k_{\text{OHc}}[\text{MOH}] + k_{\text{Oc}}[\text{MO}_2])[\text{CN}] \quad (10)$$

the concentrations of the $[\text{MO}(\text{X})(\text{CN})_4]^{m-}$, $[\text{MO}(\text{H}_2\text{O})(\text{CN})_4]^{n-}$, $[\text{MO}(\text{OH})(\text{CN})_4]^{(n+1)-}$, and $[\text{MO}_2(\text{CN})_4]^{(n+2)-}$ complexes, respectively. Zero-order kinetics with respect to $[\text{CN}]$ has been observed for cyanide and hydrogen cyanide exchange on

Table 2. Correlation between NMR, X-ray, Acid/Base, and Kinetic Data (at 298 K, $\mu = 1.5$ m) for $[\text{MO}_2(\text{CN})_4]^{n-}$ Complexes [M = Mo(IV), W(IV), Tc(V), Re(V), Os(VI)]

complex	$\text{p}K_{\text{a}1}^a$	$\text{p}K_{\text{a}2}^a$	$\delta^{17}\text{O}$ (ppm)	$\delta^{13}\text{C}$ (ppm)	$d(\text{M}=\text{O})$ (Å)	$d(\text{M}-\text{CN})^b$ (Å)	k_{aq}^c (s ⁻¹)	k_{oc}^d (s ⁻¹)
$[\text{Mo}^{\text{IV}}\text{O}_2(\text{CN})_4]^{4-}$	9.88	>14	460	170	1.834(9) ^j	2.20(1) ⁱ	4.1×10^4	$>4 \times 10^{-1}$
$[\text{W}^{\text{IV}}\text{O}_2(\text{CN})_4]^{4-}$	7.89	14.5	390	166	1.842(4) ^k	2.177(7) ^k	137 ± 5	$(4.4 \pm 0.4) \times 10^{-3}$
$[\text{Tc}^{\text{V}}\text{O}_2(\text{CN})_4]^{3-}$	2.90	4–5	578	153	—	—	500	$(4.8 \pm 0.4) \times 10^{-3}$ ^g
$[\text{Re}^{\text{V}}\text{O}_2(\text{CN})_4]^{3-}$	1.31	3.72	462	142	1.781(3) ^j	2.13(1) ^j	$(9.1 \pm 0.1) \times 10^{-2}$	$(3.6 \pm 0.3) \times 10^{-6}$
$[\text{Os}^{\text{VI}}\text{O}_2(\text{CN})_4]^{2-d}$	-3^e	$\leq 1^e$	568	120 ^f	1.75(1) ^j	2.11(1) ^j	$<10^{-8}$	$<4 \times 10^{-9}$ ^h

^a Acid dissociation constants of $[\text{MO}(\text{OH}_2)(\text{CN})_4]^{n-}$ complexes,⁶ as defined in Scheme 1. ^b Average equatorial M–CN distances obtained from X-ray studies. ^c Water exchange rate in the $[\text{MO}(\text{OH}_2)(\text{CN})_4]^{n-}$ complexes.⁷ ^d Cyanide exchange rate in the $[\text{MO}_2(\text{CN})_4]^{(n+2)-}$ complexes (this work). ^e Estimated from the $\text{p}K_{\text{a}1}$ value difference of *ca.* 4 pH units observed in $[\text{ReN}(\text{H}_2\text{O})(\text{CN})_4]^{2-}$ and $[\text{OsN}(\text{H}_2\text{O})(\text{CN})_4]^{-}$.⁷ ^f Observed $|^1J(^{187}\text{Os}-^{13}\text{C})| = 92$ Hz, a tripletlike structure where the two satellites correspond to the spin $1/2$ osmium-187. ^g At 279 K. ^h At 348 K. ⁱ Reference 15. ^j Reference 4. ^k Reference 20.

Table 3. ¹⁵N Chemical Shift Data^a for Different *trans*- $[\text{MO}(\text{X})(\text{CN})_4]^{m-}$ Complexes at 298 K [M = Tc(V), Re(V)]

complex	$\delta^{15}\text{N}$ (Tc) (ppm)	$\delta^{15}\text{N}$ (Re) (ppm)
$[\text{MO}_2(\text{CN})_4]^{3-}$	-100	-100
$[\text{M}_2\text{O}_3(\text{CN})_8]^{4-b}$	-86	-83
$[\text{MO}(\text{NCS})(\text{CN})_4]^{2-c}$	-65	—
$[\text{MO}(\text{OH}_2)(\text{CN})_4]^{-}$	-62	-61

^a Referenced relative to neat CH_3NO_2 .⁹ ^b An oxo bridging two M(V) centers.³ ^c $\delta^{15}\text{N}(\text{W}) = -190$ ppm and $|^1J(^{183}\text{W}-^{15}\text{N})| = 8$ Hz.

$[\text{ReO}_2(\text{CN})_4]^{3-}$, cyanide exchange on $[\text{TcO}_2(\text{CN})_4]^{3-}$ and $[\text{WO}(\text{OH})(\text{CN})_4]^{3-}$, and hydrogen cyanide exchange on $[\text{WO}(\text{OH}_2)(\text{CN})_4]^{2-}$ (discussion below). This implies that the observed rate constant, k_{obs} , is independent of the free cyanide concentration.

Upon inclusion of the relative acid/base ($K_{\text{a}1}$ and $K_{\text{a}2}$, reactions 4 and 6 in Scheme 1) and stability constants (K_{x} , reaction 2), the expression for the pseudo-first-order rate constant, k_{obs} (where $d[\text{M}^*\text{CN}]/dt/[\text{M}^*\text{CN}] = 4k_{\text{obs}}$), as given in eq 11, is obtained. The $[\text{WO}(\text{X})(\text{CN})_4]^{m-}$ complexes selected

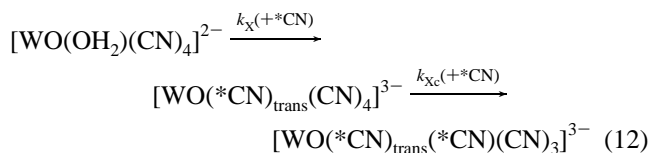
$$k_{\text{obs}} = \frac{k_{\text{CN}}}{4} = \{k_{\text{Xc}}K_{\text{x}}[\text{X}][\text{H}^+]^2 + k_{\text{aqc}}[\text{H}^+]^2 + k_{\text{OHc}}K_{\text{a}1}[\text{H}^+] + k_{\text{Oc}}K_{\text{a}1}K_{\text{a}2}\} / \{4(K_{\text{x}}[\text{X}][\text{H}^+]^2 + [\text{H}^+]^2 + K_{\text{a}1}[\text{H}^+] + K_{\text{a}1}K_{\text{a}2})\} \quad (11)$$

for study were investigated under conditions where these species were the main complexes in solution, i.e., where $[\text{H}^+] > K_{\text{a}1}$ and $K_{\text{x}}[\text{X}] \gg 1$, with the exception of the pentacyano complex; since $K_{\text{x}}[\text{X}] \gg \gg 1$ and even though a pH was used where $[\text{H}^+] \approx K_{\text{a}1}$, $[\text{WO}(\text{CN})_5]^{3-}$ was still by far the main complex in solution. Thus, under selected conditions, eq 11 can simplify to $k_{\text{obs}} = k_{\text{Xc}}/4$, which allowed selective study of the exchange rates on the $[\text{WO}(\text{X})(\text{CN})_4]^{m-}$ complexes (reaction 1 in Scheme 1).

Tungsten(IV). The W(IV) system could be studied in most detail, with a range of different monosubstituted complexes of the general form $[\text{WO}(\text{X})(\text{CN})_4]^{n-}$ included (see Table 4). The effect of the variation of the *trans* ligand X in the $[\text{WO}(\text{X})(\text{CN})_4]^{n-}$ complexes on the exchange rates of the equatorial cyano ligands is coupled with the relative M–CN bond strength as estimated from the first-order coupling between the ¹³C and the ¹⁸³W and from X-ray structural results (Table 1 and Figure 3).

Upon addition of the ¹³C-labeled cyanide in the $[\text{WO}(\text{OH}_2)(\text{CN})_4]^{2-}$ complex, there is a rapid *trans* substitution, ($k_{\text{X}} = 1 \text{ M}^{-1} \text{ s}^{-1}$),¹⁵ followed by the exchange at the equatorial

cyano sites as shown in eq 12 (also in the final spectrum in Figure 3).



Molybdenum(IV). The cyanide exchange for the pentacyano complex of Mo(IV) showed similar behavior to that observed for the W(IV) described above, i.e., the fast formation of the $[\text{MoO}(\text{CN})_5]^{3-}$ complex followed by the slower formation of the $[\text{MoO}(\text{CN})_5]^{3-}$ moiety. The results obtained from fitting the data to eq 9 are reported in Table 4.

Technetium(V). The cyanide exchange on the dioxotetracyanotechnetate(V) complex was studied by slow isotopic exchange upon introduction of C^{15}N^- rather than $^{13}\text{CN}^-$ (see discussion above) and showed well-behaved first-order kinetics (also illustrated in Figure 1). Variations of 2–3-fold in both the total cyanide as well as the $[\text{C}^{15}\text{N}]$ showed no significant change in the exchange rate in the dioxo species. The rate of exchange on the $[\text{TcO}(\text{NCS})(\text{CN})_4]^{2-}$ and $[\text{TcO}(\text{H}_2\text{O})(\text{CN})_4]^{-}$ complexes could only be estimated due to decomposition observed after 24 h (see Table 4).

Rhenium(V). The Re(V) complexes were studied by slow isotopic exchange utilizing enriched K^{13}CN and monitoring the signal growth *vs* time. The Brønsted acid/base properties of the tetracyanoaquaorhenate(V) complex (Table 2) are well defined and allowed the study of the exchange between the dioxo complex and both cyanide and hydrogen cyanide as illustrated in Figure 4 (note a $\text{p}K_{\text{a}}(\text{HCN}) = 9.2$ determined from ¹³C and ¹⁵N free cyanide chemical shift pH dependence). Three distinct features are clear from these results. First, the exchange reaction on $[\text{ReO}_2(\text{CN})_4]^{3-}$ shows a pH dependence (Figure 4) but does not correlate directly with the $\text{p}K_{\text{a}}$ value of the HCN or the protonation of either an oxo or cyano site on the complex (¹³C and ¹⁵N bound cyanide chemical shifts as a function of pH are shown in the same figure; an ¹⁷O chemical shift study also yielded similar results). Secondly, the exchange rate was independent of $[\text{CN}^-]$ at pH 11 and of $[\text{HCN}]$ at pH 6 for free ligand concentration between 0.3 and 1.6 m (see further discussion below). The third observation stems from the variable temperature study: the activation parameters determined at pH 11 differ from those determined at pH 6 where ΔH^\ddagger values are 139 ± 3 and $101 \pm 1 \text{ kJ mol}^{-1}$ and ΔS^\ddagger values are 104 ± 8 and $6 \pm 3 \text{ J K}^{-1} \text{ mol}^{-1}$, respectively (Supporting Information).

Rate Law for Cyanide Exchange on Re(V). As mentioned above, the cyanide exchange on the Re(V) dioxo complex showed a pH dependence that could not be attributed to the

(15) (a) Smit, J. P.; Purcell, W.; Roodt, A.; Leipoldt, J. G. *J. Chem. Soc., Dalton Trans.* **1995**, 1201. (b) Smit, J. P.; Purcell, W.; Roodt, A. Manuscript in preparation.

Table 4. Equatorial Cyanide Exchange Rate Constants (in s⁻¹) at 298 K (Unless Otherwise Stated) for the *trans*-[M(X)(CN)₄]ⁿ⁻ Complexes [M = Mo(IV), W(IV), Tc(V), Re(V), Os(VI)] at Various pH Values (Given in Parentheses)

complex	k_{Oc}	k_{OHc}	k_{aqc}	k_{Xc}
[MoO ₂ (CN) ₄] ⁴⁻	$>4 \times 10^{-1}$ (14.5)	$(1.7 \pm 0.1) \times 10^{-2}$ (13)	$(1.5 \pm 0.1) \times 10^{-2}$ (4.5)	
[MoO(CN) ₅] ³⁻	—	—	—	$(9.6 \pm 0.8) \times 10^{-3}$ ^c (8.9)
[WO ₂ (CN) ₄] ⁴⁻	$(4.4 \pm 0.4) \times 10^{-3}$ (14.5)	$(9.6 \pm 0.9) \times 10^{-5}$ (11.8)	$(1.1 \pm 0.1) \times 10^{-4}$ (3.1)	
[WO(CN) ₅] ³⁻	—	—	—	$(1.1 \pm 0.1) \times 10^{-2}$ ^c >4 ^{a,c} (8.8)
[WO(N ₃)(CN) ₄] ³⁻	—	—	—	$(3.1 \pm 0.2) \times 10^{-4}$ (5.5)
[WO(F)(CN) ₄] ³⁻	—	—	—	$(4.8 \pm 0.1) \times 10^{-5}$ (5.2)
[TcO ₂ (CN) ₄] ³⁻	$(4.8 \pm 0.4) \times 10^{-3}$ ^c (10.6)	$(4.0 \pm 0.14) \times 10^{-3}$ ^c (2.0)	$<4 \times 10^{-5}$ (ca. 1)	—
[TcO(NCS)(CN) ₄] ²⁻	—	—	—	$<4 \times 10^{-5}$ (ca. 0.5)
[ReO ₂ (CN) ₄] ³⁻	$(3.6 \pm 0.3) \times 10^{-6}$ (11)	$(1.6 \pm 0.4) \times 10^{-6}$ (2.5)	$<4 \times 10^{-8}$ (<1)	—
[OsO ₂ (CN) ₄] ²⁻	$<4 \times 10^{-9}$ ^d (13)	—	—	—

^a Substitution of cyanide trans to oxo. ^b Equatorial cyanide exchange on the dinuclear complex ([Re₂O₃(CN)₈]⁴⁻ (ref 3) or [Tc₂O₃(CN)₈]⁴⁻). ^c At 279 K. ^d At 348 K.

protonation of either an oxo or a cyano ligand or to the pK_a value of HCN. To accommodate this phenomenon (see discussion below), a new acid dependence (Scheme 2) possibly resulting from protonation²¹ of a cyano ligand in the [ReO₂(CN)₄]³⁻ complex or an outer-sphere interaction of a cyano moiety, [ReO²(CN)₄]³⁻, is defined. This will be discussed in further detail below.

The rate law given in eq 15 can therefore be derived.

$$d[M^*CN]/([M]dt) = \frac{k_{OCH}[H^+] + k_{Oc}K_{a3}}{[H^+] + K_{a3}} \quad (15)$$

Upon fitting the data points (Figure 4), a k_{OCH} of $(1.2 \pm 0.4) \times 10^{-4}$ s⁻¹ is obtained compared to a k_{Oc} of $(3.6 \pm 0.3) \times 10^{-6}$ s⁻¹ (Table 4).

Osmium(VI). It has previously been concluded that even in strong acid solution, the dioxotetracyanoosmate(VI) complex cannot be protonated to form the oxo aqua complex or even the corresponding hydroxo oxo complex. The pK_{a1} and pK_{a2} values have been estimated to be substantially less than 1.^{4,22}

An extreme slow kinetic behavior, as expected for the +6 charged metal center for a dissociative activation exchange process, has been observed. An upper limit for the oxygen exchange has been determined (Table 2), and the results for cyanide exchange, determined from fitting the data to eq 9,²³

yielded a k_{CN} of $<4 \times 10^{-9}$ s⁻¹ at pH 13 and of $(1.2 \pm 0.1) \times 10^{-4}$ s⁻¹ at pH 2.5.

Discussion

Correlation between Structural Results and [¹J(¹⁸³W—¹³C)]. The correlation between the X-ray crystallographic data of the W—CN bond lengths and the first-order coupling constants between the ¹⁸³W and ¹³C in the equatorial cyano ligands, as predicted by the Fermi contact term,²⁴ is fairly good (see Table 1). This illustrates the increase in W—CN cis bond length induced by increased donor strength of the trans ligand. Furthermore, the increase in stability constants (pK_x = -log K_x, K_x = stability constant) of the relevant [WO(X)(CN)₄]ⁿ⁻ complexes, as a function of ligand strength, is also in good agreement with this effect.

The equatorial M—CN bond length decreases from the W(IV) dioxo complex to the hydroxo and aqua related complexes by 2.18 to ca. 2.14 Å, respectively (see Table 1), which corresponds to an observed increase of about 10 Hz in the coupling constant. It is interesting to note the significant increase in M—CN bond length induced by the two oxo ligands forming the trans O=M=O moiety. The introduction of the two double bonds trans to each other introduces substantial electron density to the metal center, resulting in lengthening of the equatorial M—CN bonds. This weakening of the cyano bonds is well manifested in the ca. 2–3 order increase observed in the CN exchange rate constants for all the systems (see also further discussion below) and is in good agreement with a dissociative mechanism for the cyanide exchange in general for these metal centers.

(16) Wieghardt, K.; Backes-Dahman, G.; Holtzbach, W.; Swiridoff, W. J.; Weiss, J. Z. *Anorg. Allg. Chem.* **1983**, 499, 44.

(17) Robinson, P. R.; Schlemper, E. O.; Murmann, R. K. *Inorg. Chem.* **1995**, 14, 2035.

(18) Leipoldt, J. G.; Basson, S. S.; Roodt, A.; Potgieter, I. M. S. *Afr. J. Chem.* **1986**, 39, 179.

(19) Basson, S. S.; Leipoldt, J. G.; Potgieter, I. M.; Roodt, A. *Inorg. Chim. Acta* **1985**, 103, 121.

(20) Roodt, A. Unpublished work.

(21) Sotomayor, J.; Parola, A. J.; Pina, F.; Zinato, E.; Riccieri, P.; Manfrin, M. F.; Moggi, L. *Inorg. Chem.* **1995**, 34, 6532.

(22) van der Westhuizen, H. J.; Basson, S. S.; Leipoldt, J. G.; Purcell, W. *Polyhedron* **1994**, 13, 717.

(23) In the case of the Os(VI) ¹⁷O NMR study, the estimation of the rate of exchange was determined from the peak height of the coordinated oxygen-17 water as a function of time using the following form of eq 3: $h = h_{\infty}(1 - \exp[-k_{\text{obs}}t])$, where x and x_{∞} , being small, are proportional to h and h_{∞} , respectively, and $(1 - x_{\infty})$ in the above exponential term is ≈ 1 due to the large free H₂O signal.

(24) Steyn, G. J. J.; Roodt, A.; Osetrova, G.; Varshavsky, Y. S. J. *Organomet. Chem.* **1997**, 536/537, 197.

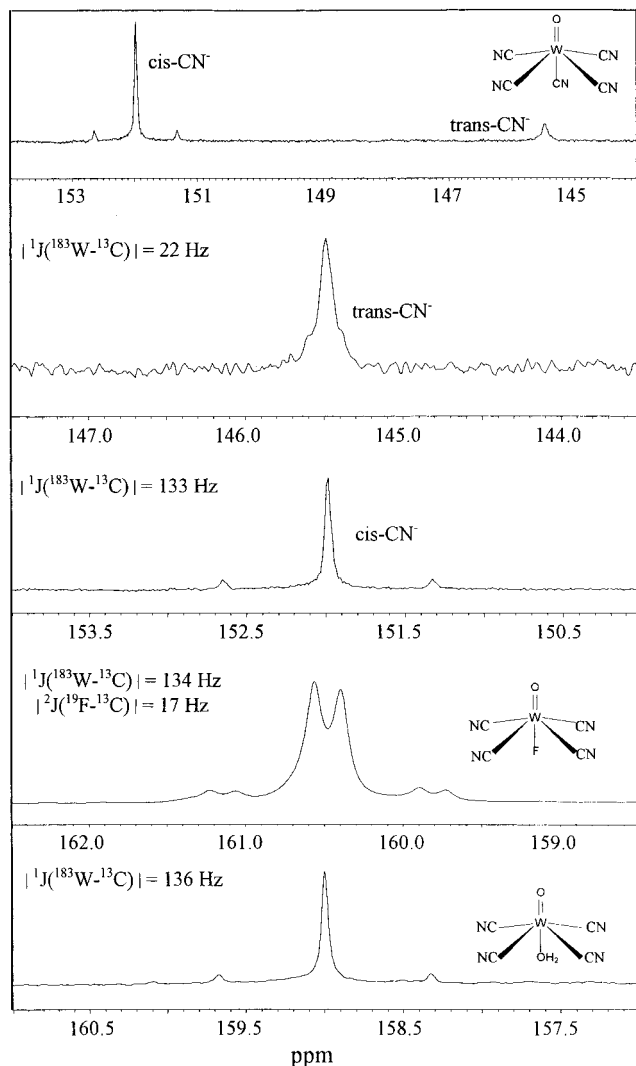


Figure 3. ^{13}C NMR spectra for $[\text{WO}(\text{X})(^{13}\text{CN})_4]^{n-}$ illustrating the variation in chemical shift ($\delta[\text{Re}_2\text{O}_3(\text{CN})_8^{4-}] = 134$ ppm, external reference¹²) and $|^1J(^{183}\text{W}-^{13}\text{C})|$ coupling constants for $[\text{WO}(^{13}\text{CN})_5]^{3-}$ ($[\text{W}(\text{IV})]_{\text{tot}} = 0.2$ m, $[\text{CN}^-]_{\text{free}} = 0.3$ m, pH = 8.8); $[\text{WO}(\text{F})(^{13}\text{CN})_4]^{3-}$ ($[\text{W}(\text{IV})]_{\text{tot}} = 0.2$ m, $[\text{CN}^-]_{\text{free}} = 0.3$ m, $[\text{KF}]_{\text{tot}} = 0.33$ m, pH = 5.2); and $[\text{WO}(\text{H}_2\text{O})(^{13}\text{CN})_4]^{2-}$ ($[\text{W}(\text{IV})]_{\text{tot}} = 0.2$ m, $[\text{CN}^-]_{\text{free}} = 0.3$ m, pH = 3.1).

The chemical shift of the equatorial ^{13}CN ligands in the $[\text{WO}(\text{X})(\text{CN})_4]^{n-}$ complexes does not show a systematic correlation, which is to be expected considering the significant differences in the electronic environment introduced to the metal center and therefore on the ^{13}C cyano nuclei due to the different trans X ligands such as F^- , pyridine, NCS^- , CN^- , aqua, OH^- , and O^{2-} (also see Table 1). It is, however, interesting to note that the equatorial ^{13}C chemical shift in the $[\text{WO}(\text{CN})_5]^{3-}$ complex is 152 ppm compared to the other $[\text{MO}(\text{X})(\text{CN})_4]^{n-}$ complexes with chemical shifts of 162, 161, 157, 159, 159, and 159 ppm for X = OH^- , F^- , N_3^- , NCS^- , py, and H_2O , respectively. The significant downshift in the frequency for the pentacyano complex relative to the others is worth noting and might be related to the enhanced exchange rate of the pentacyano complexes compared to the other $[\text{MO}(\text{X})(\text{CN})_4]^{n-}$ complexes (see further discussion below).

Of significance is the result obtained from ^{99}Tc NMR as illustrated in Figure 2. The chemical shift of the $[\text{H}_2\text{O}(\text{CN})_4]^{4-}$ ($\delta = -1350$ ppm) is the most shielded reported for a Tc(V) complex to date, the previous lowest shift being for the $[\text{H}_2\text{O}_2(\text{CN})_4]^{2-}$ ($\delta = +806$ ppm), shown in

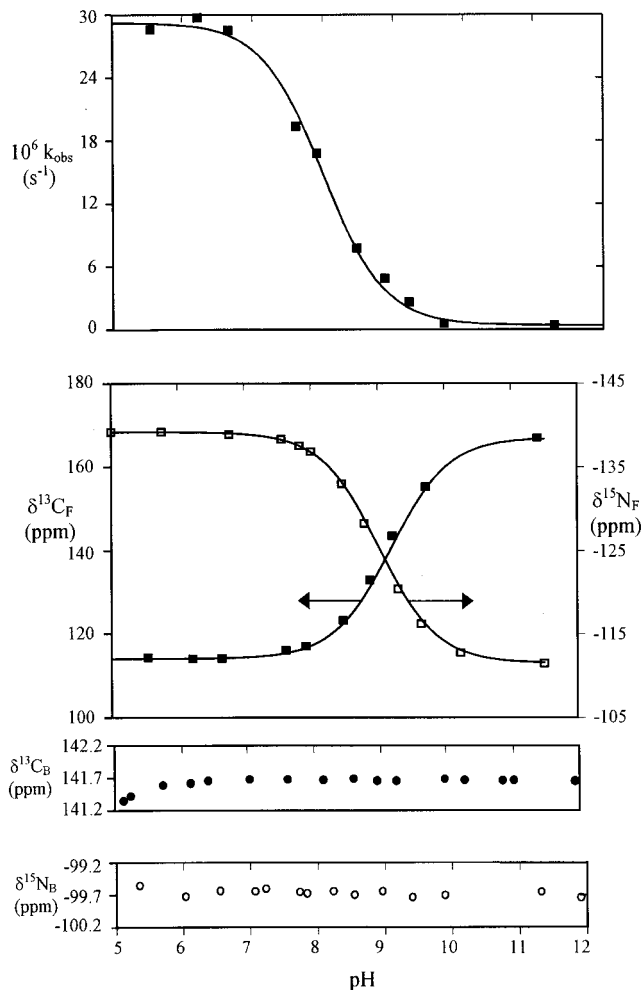


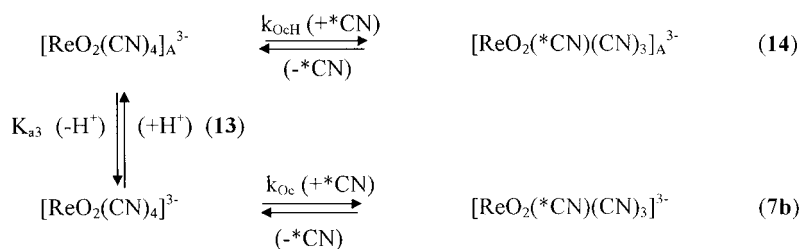
Figure 4. pH dependence of cyanide exchange rate on $[\text{ReO}_2(\text{CN})_4]^{3-}$; $\delta^{13}\text{C}_\text{F}$ and $\delta^{15}\text{N}_\text{F}$ chemical shifts of the free HCN/CN^- and $\delta^{13}\text{C}_\text{B}$ and $\delta^{15}\text{N}_\text{B}$ chemical shifts of the bound CN^- . $[\text{Re}(\text{V})]_{\text{tot}} = 0.2$ m; $[\text{HCN}/\text{CN}^-] = 0.3$ m; $T = 25$ °C; $\mu = 1.5$ – 2.8 m.

Figure 2. This observation underlines the fact that the oxidation state of a Tc center cannot be directly estimated (other than perhaps for the identification of Tc(I) complexes) from the ^{99}Tc chemical shift, as has been suggested previously.^{10b,c}

Exchange Kinetics. Exchange on Dioxo Complexes. The cyanide exchange rates, k_{oc} , for the range of dioxotetracyano-metalate complexes of Mo(IV), W(IV), Tc(V), Re(V), and Os(VI) shows the following trend: $\text{M}(\text{IV}) > \text{M}(\text{V}) > \text{M}(\text{VI})$, which is in direct agreement with the acid/base behavior of these oxidation states and also in excellent agreement with the M–CN bond lengths of the corresponding oxidation states, as illustrated in Table 2. The ca. 2–3 orders of magnitude difference observed for the cyanide exchange between the different oxidation states of the metal center is significant, i.e., around 10^{-1} – 10^{-3} s^{-1} for the M(IV) complexes, to ca. 10^{-3} – 10^{-6} s^{-1} for the M(V) and $<10^{-9}$ s^{-1} for the M(VI). This observation is in direct agreement with a dissociative activation for the cyanide exchange on these dioxo complexes. The same trend is observed upon comparison of the water exchange rate constants for these $[\text{MO}(\text{OH}_2)(\text{CN})_4]^{n-}$ complexes.

It is furthermore clear upon comparison of the coupling constants/bond strengths of the $[\text{MO}_2(\text{CN})_4]^{4-}$ and the $[\text{MO}(\text{X})(\text{CN})_4]^{n-}$ complexes in Table 1 for the W(IV) and Mo(IV), that the *trans*-dioxo core causes an elongation of the equatorial metal *cis*-cyano bonds. This results in an increase in dissociating ability for the cyano ligands, which in turn is

Scheme 2



directly reflected in the *ca.* 2 order of magnitude increase in exchange for all the dioxo complexes compared to $[\text{MO}(\text{X})(\text{CN})_4]^{n-}$ complexes, with $\text{X} \neq \text{O}^{2-}$ (see Table 4). This further points to a dissociative activation for the cyanide exchange process.

This conclusion on the activation mode for the cyanide exchange is further manifested by the results obtained for the Re(V) center whereby a 5-fold variation in free cyanide, $[\text{CN}^-]$, showed no effect on the exchange rate on the dioxo complex (see "Kinetics and Data Treatment" section and Supporting Information). This, together with the results obtained upon a 4-fold variation of $[\text{CN}^-]$ for the $[\text{TcO}_2(\text{CN})_4]^{3-}$ and $[\text{WO}(\text{OH})(\text{CN})_4]^{3-}$ complexes, further confirms the assignment of a D mechanism for the cyanide exchange on these metal centers when containing either one (classic 16-electron complexes) or two (18-electron complexes) oxo ligands. The positive value of the entropy of activation of $+104 \pm 8 \text{ J K}^{-1} \text{ mol}^{-1}$ determined in the case of the $[\text{ReO}_2(\text{CN})_4]^{3-}$ complex is further evidence of a D mechanism for the CN^- exchange in these complexes (see discussion below).

The significant reactivity difference observed for the Tc(V) and Re(V) of >4000 is in general agreement with that found in previous complex formation and oxygen exchange studies.^{4,7,25} As a result, a D mechanism is concluded for the equatorial exchange, implying that a dissociative activation also holds for strong π ligands such as cyano complexes and isocyanide moieties, the latter currently being employed for heart imaging in $^{99\text{m}}\text{Tc}$ -Sestamibi, i.e., $[\text{MIBI}]_6^+$, MIBI = methoxyisobutyl isocyanide.²⁶ On the other hand, the extreme slow exchange (half-life > 20 h) for the equatorial cyano ligands observed in this study, especially when the dioxo moiety is eliminated to yield only the mono oxo $\text{M}=\text{O}$ core, indicates that for cerebral agents such as $[\text{M}(\text{HMPAO})]_0^0$ (HMPAO = propylene amine oxime),²⁶ absorption in the brain might not be due to dissociation of the ligand but rather to outer-sphere ligand-biological host interactions or trans oxo addition/substitution of coordinated H_2O . These aspects will be further investigated in the future.

We now turn to the change in exchange rate observed for the Re(V) center as a function of pH around 8 (Figure 4), which is presented in Scheme 2; it cannot be explained unambiguously at this point in time. A similar situation existed in a recent study of the aquation of $[\text{Cr}(\text{CN})_6]^{3-}$, wherein an intermediate of the form $[\text{Cr}(\text{HCN})(\text{CN})_5]^{2-}$ was postulated as a reactive species undergoing the hydrolysis process.²¹ Similar to this mentioned study, the increase in exchange rate observed for the $[\text{ReO}_2(\text{CN})_4]^{3-}$ cannot be without doubt linked to the protonation of either an oxo or a cyano ligand, since protonation of the oxo site is well established.⁴ Furthermore, strange protonation behavior was observed at intermediate pH values

for the Re(V) complex in our previous studies.⁷ However, no change in the ^{13}C chemical shift of the coordinated cyano ligands could be detected (see Figure 4), in principle excluding protonation of a coordinated cyano ligand, provided that a chemical shift change can indeed be detected. Also when we turn to the results obtained from the ^{15}N NMR measurements in the current study, there seems to be no real indication of a tendency of a chemical shift *vs* pH dependence around pH = 8. Moreover, ^{17}O NMR chemical shift measurements did not reveal any pH dependence between pH 6 and 11. However, there does not necessarily have to be an observed change in the chemical shifts since, in the case of the Mo(IV) center, although both the $[\text{MoO}(\text{CN})_5]^{3-}$ and the $[\text{MoO}(\text{HCN})(\text{CN})_4]^{2-}$ species have been crystallographically^{3j,16} and kinetically³ⁱ verified, no NMR evidence in terms of chemical shift differences in the ^{13}C spectra could be detected. It is also of interest to note a reduction of the pK_a of the bound HCN to 7.6 for this Mo(IV) complex. A similar effect, i.e., a decrease in the pK_a of the bound HCN was observed in both $[\text{MO}(\text{HCN})(\text{CN})_4]^{2-}$ $\{\text{M} = \text{Mo}(\text{IV}), \text{W}(\text{IV})\}^{15\text{a}}$ and $[\text{ReN}(\text{HCN})(\text{CN})_4]^{2-}$ ^{3m} complexes.

A further, more unlikely process occurring to account for this observed accelerated exchange can in principle be attributed to the formation of an outer-sphere complex between the $[\text{ReO}_2(\text{CN})_4]^{3-}$ and the neutral HCN. In the reactions of cyanide with Ni(II) complexes,²⁸ HCN was postulated to be a reactant as well as CN^- but no spectral or kinetic evidence was observed. In the case of the Re(V) complex, although no NMR evidence could be gathered to suggest this, the different activation parameters determined at pH 11 and 6 indicate different operating mechanistic pathways. However, it is worth while to note that, although the exchange of the HCN compared to the CN^- is not directly related to the pK_a value of HCN, the 30-fold increase in the exchange on the Re(V) center at pH = 6 compared to pH = 11 is indeed significant. A neutral entity like HCN will exhibit much better outer-sphere interaction with the trivalent negatively charged $[\text{ReO}_2(\text{CN})_4]^{3-}$ than the negatively charged CN^- ion. It is also anticipated that the cyano ligands coordinated to the Re(V) center in the dioxo complex will be much more basic (much longer $\text{M}-\text{CN}$ bonds, see Table 2) than in the protonated oxo hydroxo or oxo aqua complexes, suggesting that this $\text{M}-\text{CN}\cdots\text{H}$ interaction might be unfavorable upon the protonation of an oxo ligand.

Cyanide Exchange in Protonated and Substituted Complexes. The exchange on the protonated $[\text{MO}(\text{H}_2\text{O})(\text{CN})_4]^-$ and $[\text{MO}(\text{OH})(\text{CN})_4]^-$, as well as the monosubstituted complexes, $[\text{MO}(\text{X})(\text{CN})_4]^{n-}$ compared to the dioxo complexes described above, shows a similar cyanide exchange pattern (Table 4). The substantial variation of the X ligands does not manifest any significant change in exchange rate constants for a specific metal center. There is, for example, only a 6-fold variation in the exchange rate constants for the range of X ligands in the W(IV) complexes, suggesting that the cis activation of the equatorial

(25) Botha, J. M.; Roodt, A. Manuscript in preparation.

(26) Jurisson, S.; Berning, D.; Jia, W.; Ma, D. *Chem. Rev.* **1993**, 1137 and references within.

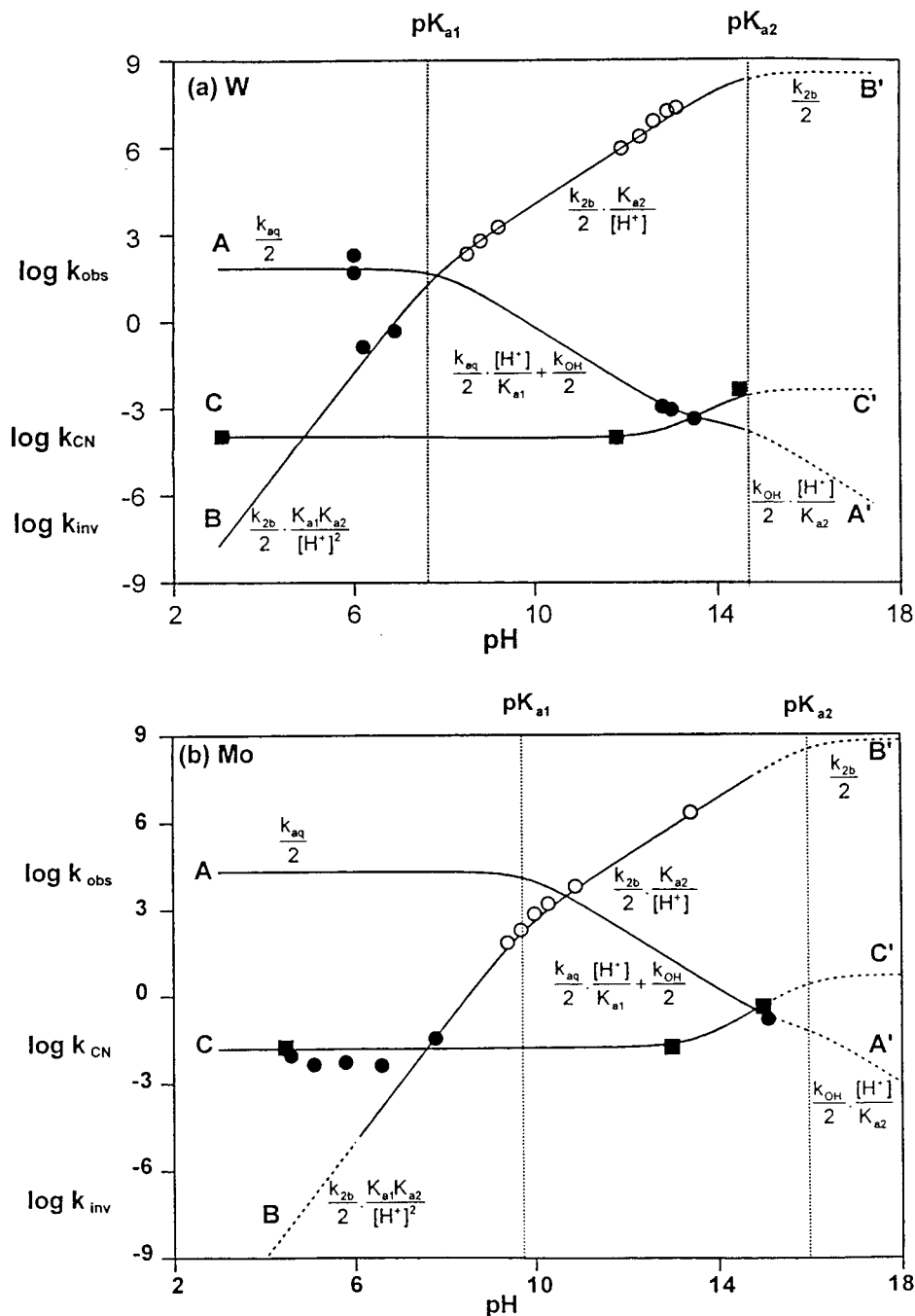


Figure 5. Correlation between the rates of inversion of the metal center along the M=O axis, with oxygen and cyanide exchange as a function of pH for (a) W(IV) and (b) Mo(IV) at 25 °C. Line AA' calculated from eq 18 gives the observed oxygen exchange rate. Line BB' calculated from eq 20 gives the observed inversion rate. Line CC' calculated from eq 11 gives the observed *cis*-cyanide exchange rate. Open and solid circles represent the ^{17}O line-broadening and isotopic exchange data points, respectively, whereas the solid squares represent the ^{13}C isotopic exchange data points.

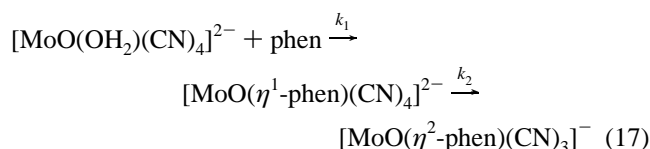
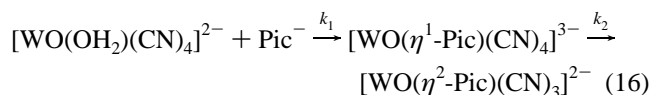
cyano ligands only shows a significant effect when a second oxo ligand on the metal center is generated via deprotonation.

Of interest to note is that in previous studies, the kinetics of the substitution reactions with bidentate ligands as shown in eqs 16 and 17 have been reported, with $\text{Pic}^- =$ pyridine-2-carboxylate^{3h} and $\text{phen} =$ 1,10-phenanthroline.²⁷

This current study showed that the cyanide exchange rate constants for a range of $[\text{WO}(\text{X})(\text{CN})_4]^{n-}$ are 10^{-4} – 10^{-5} s⁻¹.

(27) Leipoldt, J. G.; Basson, S. S.; Potgieter, I. M.; Roodt, A. *Inorg. Chem.* **1987**, 26, 57.

(28) (a) Kolski G. B.; Margerum, D. W. *Inorg. Chem.* **1968**, 7 (11), 2239. (b) Kolski, G. B.; Margerum, D. W. *Inorg. Chem.* **1969**, 8 (5), 1125. (c) Pearson, R. G.; Sweigart; *Inorg. Chem.* **1970**, 9, 1167. (d) Billo, E. G. *Inorg. Chem.* **1973**, 12 (12), 2783.



In the bidentate reaction illustrated in eq 16, the ring closure (second step) was found to be 5×10^{-4} s⁻¹ under normalized conditions (same ligand concentration as in the current study),

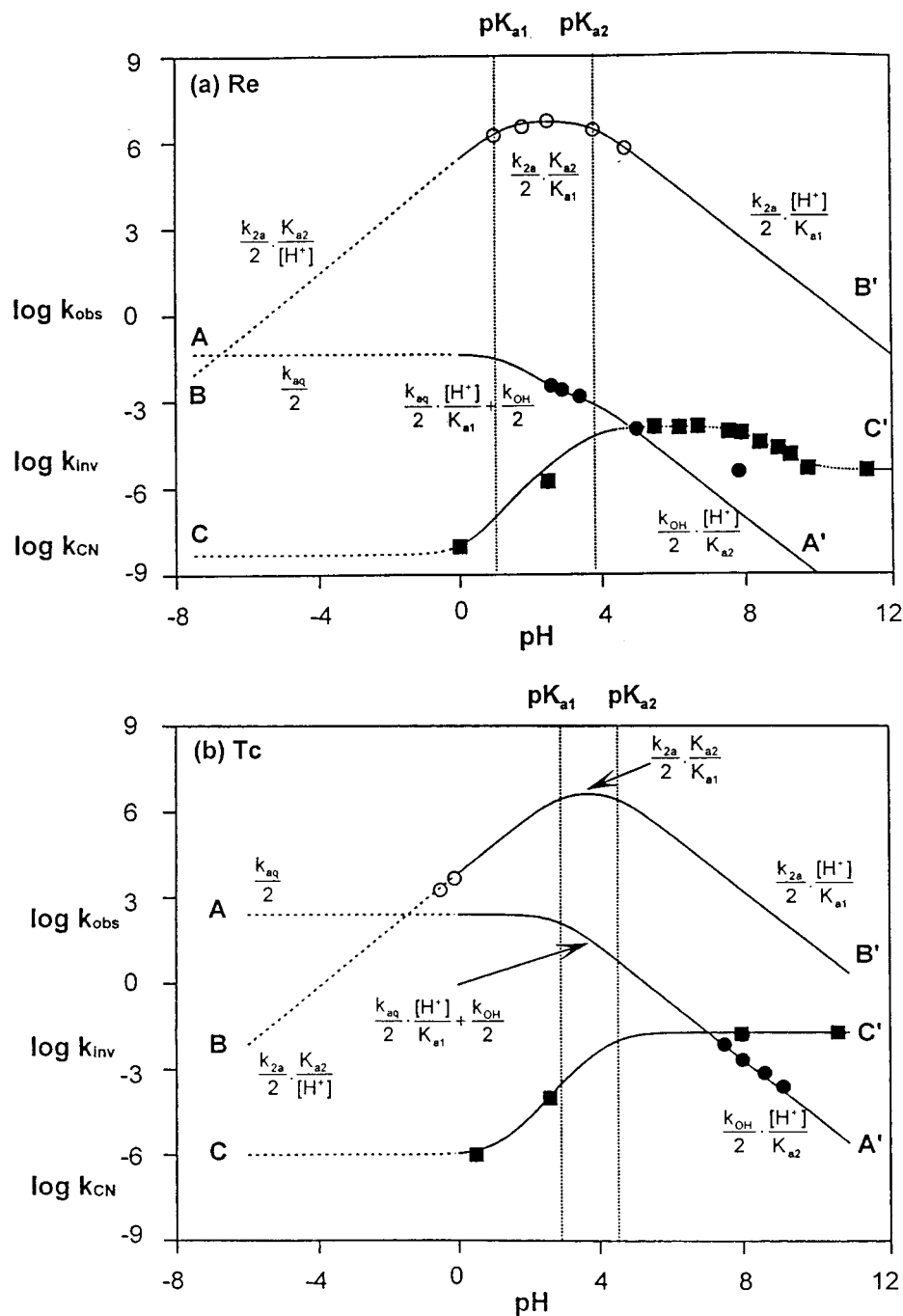


Figure 6. Correlation between rates of inversion of metal center along the $M=O$ axis, with oxygen and cyanide exchange as a function of pH for (a) Re(V) and (b) Tc(V) at 25 °C. Line AA' calculated from eq 18 gives the observed oxygen exchange rate. Line BB' calculated from eq 19 gives the observed inversion rate. Line CC' calculated from eq 11 for Tc(V) and from eq 15 for Re(V) gives the observed *cis*-cyanide exchange rate. Open and solid circles represent the ^{17}O line-broadening and isotopic exchange data points, respectively, whereas the solid squares represent the ^{15}N and ^{13}C isotopic exchange data points.

which is exactly the same as the equatorial cyanide exchange rate determined in this current study. This confirms that the second step in eq 16 indeed represents the ring closure (i.e., substitution of a cyano ligand) which is *ca.* 3 orders of magnitude slower than the initial aqua substitution. The rate constant k_1 in eq 16 is comparable to the substitution rates obtained for monodentate ligands of *ca.* $1-10\text{ s}^{-1}$, i.e., formation of the $[\text{WO}(\text{X})(\text{CN})_4]^{n-}$ complexes. Similarly, the reaction rate obtained in the study on the Mo(IV) center illustrated in eq 17, i.e., $4 \times 10^{-2}\text{ s}^{-1}$, for the ring closure process, is in excellent agreement with the equatorial cyanide exchange rates of *ca.* 10^{-3} s^{-1} determined for the Mo(IV) center in the current study.

This ring closure (and equatorial cyanide substitution) is much slower than the aqua substitution of *ca.* 100 s^{-1} found for formation of the pentacyano complex of Mo(IV).

A further interesting observation from the current study relates to the fact that the cyanide exchange rate constants for the equatorial CN ligand in the pentacyano complexes of both the W(IV) and Mo(IV) are *ca.* 2–3 orders of magnitude faster than for the protonated complexes and less pronounced for the Mo(IV) (only *ca.* 4-fold increase) complexes (see Table 4). This cannot be explained at this point, but it is quite possible to be linked to an intramolecular rearrangement of the $^{13}\text{CN}^-$ (trans to the oxo) already coordinated to the metal center. Instead of

the exchange process proceeding via complete dissociation and then re-coordination, an intramolecular rearrangement is possible without the $^{13}\text{CN}^-$ leaving the primary coordination sphere. As mentioned above, the significant difference in chemical shift observed for the *cis*-CN in the pentacyano complexes relative to the other species might be an indication of different electron density distributions as a result of significant π interactions by the five cyano ligands on the metal center favoring this postulated intramolecular rearrangement. This rearrangement/isomerization, however, has to be associated with a process involving the equatorial cyano bond re-organization/breaking/rearrangement as rate-determining step and is not determined by the breaking of the *trans* M–CN bond, since the hydrolysis rate constants for the decomposition of the oxo pentacyano complex to the corresponding aqua oxo tetracyano moieties were determined as 200^{31} and 8^{15} s^{-1} for the Mo(IV) and W(IV), respectively. This is *ca.* 2–3 orders of magnitude larger than the equatorial exchange observed in the current study and implies that the exchange process should have been much faster if the rate-determining step was directly related to the cleavage of the M–C bond in the *trans* O=M–CN moiety.

The data for the $[\text{MO}(\text{X})(\text{CN})_4]^{n-}$ complexes for Re(V) ($\text{X} = \text{OH}^-, \text{OH}_2$) and Tc(V) ($\text{X} = \text{OH}_2, \text{NCS}^-$) are unfortunately limited but show that the Re(V) center is much less reactive (by about 3 orders of magnitude) than the corresponding Tc(V) complexes, thus confirming the general trends observed for the M(IV) metal centers.

Correlation between Proton, Oxygen, and Cyanide Exchange. The different exchange processes studied previously and in the current work are combined on maps of reactivity vs pH relationship (Figure 5, Mo(IV) and W(IV); Figure 6, Tc(V) and Re(V)) for the individual metal centers, which were constructed as follows.

(a) Cyanide exchange: eq 11 (Mo(IV), W(IV), Tc(V), and Os(VI)) and eq 15 (Re(V)).

(b) Oxygen exchange: eq 18 for all the metal centers; this equation is derived from previous studies⁷ for the oxygen exchange on these metal centers where it was shown that the dioxo species did not undergo any detectable oxygen exchange other than via acid-catalyzed pathways for all the studied complexes.

$$k_{\text{obs}} = \frac{(k_{\text{aq}} + k_{\text{OH}}K_{\text{a1}}/[\text{H}^+])}{2(1 + K_{\text{a1}}/[\text{H}^+] + K_{\text{a1}}K_{\text{a2}}/[\text{H}^+]^2)} \quad (18)$$

(c) Proton exchange: eq 19 (for Mo(IV) and W(IV)) and eq 20 (for the Re(V) and Tc(V)). In fact, the proton exchange for the M(V) centers, as manifested by the inversion induced on the coordination polyhedron via protolysis, is described by eq 19, as was shown previously.⁷

$$k_{\text{inv}} = (k_{2\text{a}}K_{\text{a1}}/2[\text{H}^+])/[(1 + K_{\text{a1}}/[\text{H}^+] + K_{\text{a1}}K_{\text{a2}}/[\text{H}^+]^2)] \quad (19)$$

Similarly, the corresponding function describing the inversion of the coordination polyhedron via hydrolysis for the M(IV) systems (Mo(IV) and W(IV)) was previously⁷ derived and is given in eq 20.

$$k_{\text{inv}} = (k_{2\text{b}}K_{\text{a2}}K_{\text{a1}})/2[\text{H}^+]^2/(1 + K_{\text{a1}}/[\text{H}^+] + K_{\text{a1}}K_{\text{a2}}/[\text{H}^+]^2) \quad (20)$$

It is significant that the reactivity behavior for all four metal centers is described over a *ca.* 10-order of magnitude range. Although these are certainly wider than practical pH ranges, they illustrate a wider interpretation of all the data and are of theoretical interest. The cyanide exchange processes are in most cases the slowest. However, it is interesting to note that for the Mo(IV) center specifically, the previously unexplained more rapid than expected oxygen exchange at pH values lower than 6 might be associated with the cyanide exchange being more rapid. It is quite possible that the rapid decomposition observed for the aqua oxo complex of Mo(IV) at these pH values is due to hydrolysis stimulated by the relative rapid cyanide exchange at this acidity.

Another interesting observation stems from the slight deviation observed for the Re(V) system at $\text{pH} > 6^7$ as illustrated in Figure 6, for the oxygen exchange and the seemingly unexplained pH dependence for the CN exchange around $\text{pH} 6\text{--}9$. Around these pH values, the oxygen exchange and the cyanide exchange rates are quite similar. Therefore, it is reasonably assumed that the two exchange processes may be linked to similar intermediates. This will be further investigated in the future.

To conclude, in this paper we have combined previously studied subjects of these metal centers to allow construction of different relationships as illustrated in Figures 5 and 6. Using this range of metal centers, different aspects were studied in terms of reactivity, structural, and general spectroscopic characteristics. Future studies to implement some of the knowledge obtained in this work are planned in the aim of designing complexes with potential application in the radiopharmaceutical industry.

Acknowledgment. Financial support for this research, provided by the Swiss National Science Foundation (Grant No. 2039483.93), is gratefully acknowledged. A.R. also thanks the Research Fund of the University of the Orange Free State and the South African FRD for financial assistance. Dr. J. M. Botha from the UOFS is thanked for part of the synthetic work.

Supporting Information Available: Tables of the observed rate constants for the slow isotopic ^{13}C , ^{15}N , and ^{17}O exchange as well as the calculated inversion rates, cyanide kinetic data, and oxygen and cyanide exchange constants are available (3 pages). Ordering information is given on any current masthead page.

IC971239S